Infrared Observations of the Orion Capsule During EFT-1 Hypersonic Re-entry

Thomas J. Horvath[1], Shann J. Rufer[2], and David M. Schuster[3]
NASA Langley Research Center, Hampton VA 23681
Gavin F. Mendeck[4], and A. Brandon Oliver[5],
NASA Johnson Spaceflight Center, Houston TX 77058
Richard J. Schwartz[6]
Analytical Mechanics Associates, Hampton, VA 23681
Harry A. Verstynen[7]
Unisys Corporation, Hampton, VA 23681
C. David Mercer[8]
Stinger Graffarian Technologies, VA 23681
Steven Tack[9] and Ben Ingram[10]
Naval Air Warfare Center - Weapons Division, Pt. Mugu, CA 93042
Thomas S. Spisz[11], Jeff C. Taylor[12], David M. Gibson[13], Kwame Osei-Wusu[14], and Steve Kennerly[15]
Johns Hopkins University Applied Physics Laboratory, Laurel, MD 20723
Brett Bush[16]
Raytheon/Photon Research Associates, San Diego, CA 92121

High-resolution infrared observations of the Orion capsule during its atmospheric reentry on December 5, 2014 were made from a US Navy NP-3D. This aircraft, equipped with a long-range optical sensor system, tracked the capsule and imaged its heat shield from Mach 10 to 6 from distances of approximately 60-45 nmi. Global surface temperature of the capsule's thermal heat shield were derived from near infrared intensity measurements. The global surface temperature measurements complemented onboard instrumentation and were invaluable to the interpretation of the sub-surface thermocouple measurements that rely on inverse heat transfer methods and material response codes to infer the desired surface temperature from the sub-surface measurements. The paper describes the motivations behind the NASA Engineering Safety Center sponsored observation and highlights the subsequent pre-mission planning process of the Scientifically Calibrated In Flight Imagery (SCIFLI) team with an emphasis on aircraft placement, optimal instrument configuration and sensor calibrations. Critical aspects of SCIFLI mission operations coordinated from the NASA Johnson Spaceflight Center and integration with the NASA Johnson Flight Test Management Office are presented. A summary of the imagery that was obtained and processed to global surface temperature is presented. At the capsule's point of closest approach relative to the imaging system, the spatial resolution of the thermal imagery was estimated to be approximately 12-15-inches per pixel. Image post processing improved the effective resolution and was sufficient to identify localized temperature increases associated with compression pad support hardware on the heat shield. Comparisons are made between surface temperature

[1] Aerospace Engineer, LaRC Aerothermodynamics Branch, AIAA Associate Fellow.
[2] Aerospace Engineer, LaRC Aerothermodynamics Branch.
[3] Lead, Aerosciences Technical Discipline Team, NASA Engineering Safety Center.
[4] Orion Entry, Descent & Landing Phase Engineer, JSC.
[5] Aerospace Engineer, JSC Applied Aeroscience and CFD Branch.
[6] Aerospace Engineer, LaRC Advanced Sensing and Optical Measurement Branch.
[7] Former LaRC Chief Test Pilot (NASA Ret).
[8] Aerospace Engineer, LaRC Structural Mechanics and Concepts Branch.
[9] Lead, Cast Glance Electro-Optical Systems and Flight Operations.
[10] Imaging Specialist, Cast Glance Electro-Optical Systems and Flight Operations.
[11] Senior Professional Staff, Applied Physics Laboratory, JHU.
[12] Principal Professional Staff, Applied Physics Laboratory, JHU.
[13] Principal Professional Staff, Applied Physics Laboratory, JHU.
[14] Senior Professional Staff, Applied Physics Laboratory, JHU.
[15] Senior Professional Staff, Applied Physics Laboratory, JHU.
[16] Senior Professional Staff, Raytheon.

reconstructed from sub-surface thermocouples to image-derived global surface temperature. The two complimentary measurements serve as an example of the effective leveraging of resources to advance the understanding of high Mach number environments associated with an ablated heat shield and provide unique data for the validation of design tools and numerical flight simulation techniques.

1. Introduction

The Exploration Flight Test 1 (EFT-1) of the Orion Multi-Purpose Crew Vehicle occurred with a successful launch on December 5, 2014. The uncrewed flight test was designed to collect vital measurements in flight that will influence future design decisions associated with the follow-on crewed flights within the next decade. The data collected was intended to permit engineers to reduce risk and costs by more accurately assessing existing performance margins and validation of existing engineering and numerical design methods. A Delta IV Heavy upper stage took the EFT-1 capsule to an altitude of approximately 3,600 miles above the Earth's surface, more than 15 times farther than the International Space Station's (ISS) orbital position. Flying out to and returning from these distances, engineers were able to begin to determine how the capsule will perform when returning from future deep space journeys to the moon and beyond.

The EFT-1 mission was a 4.5 hour, two orbit flight test of the Orion capsule and its subsystems, concluding with a high-energy reentry (~80% of lunar return velocity) during early daylight conditions over the Pacific. One of the critical objectives during the flight test was to evaluate the ability of the heat shield thermal protection system (TPS) to protect the capsule structure and other important crew module hardware from the intense heat generated during reentry. The Orion heat shield was predominantly made of Avcoat, an ablative material similar to the formulation used on the Apollo command module capsules over four decades ago. While much smaller than the Shuttle that it is to replace, the Orion capsule's monolithic heat shield was the largest of its kind ever built with a diameter of 16.5 feet and a thickness of approximately 1.6 inches. During the reentry phase of the flight test, the heat shield surface temperature was expected to peak at approximately 4000° F, higher than that experienced on the acreage non-ablating ceramic TPS tiles of the now retired Space Shuttle when returning from the ISS in low earth orbit.

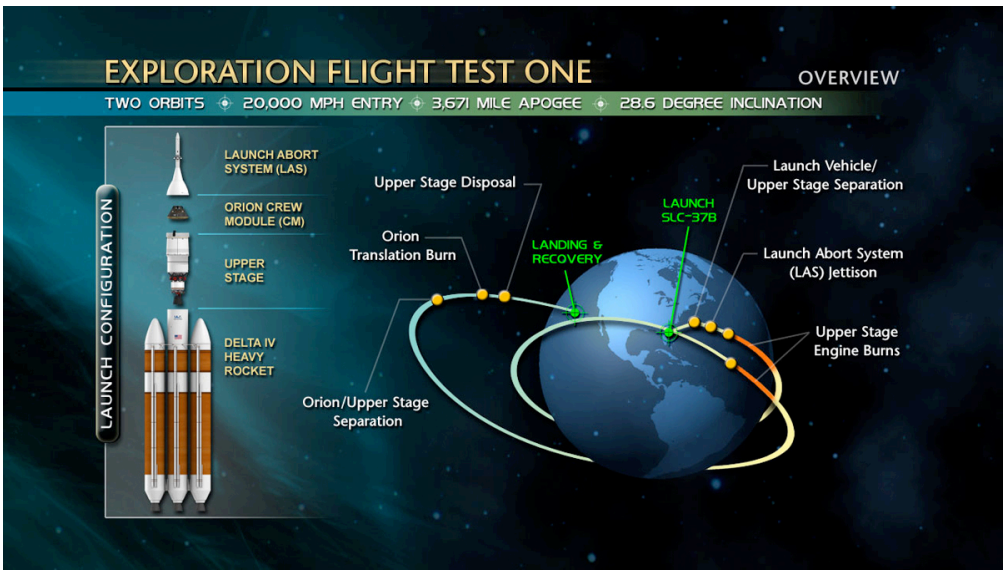

Figure 1-1. EFT-1 Flight Test

As part of the flight test, spatially resolved infrared imagery of the capsule heat shield during its return back to earth was desired to compliment surface temperature reconstructed from a limited number of sub-surface thermocouples. Drawing upon the success of previous thermal observations [Refs. 1-20], the Scientifically Calibrated In Flight Imagery (SCIFLI) team formed the nucleus of a NASA Engineering Safety Center (NESC) assessment team whose objective was to determine if such an observation with the dimensionally smaller and hotter capsule was possible, and if so, assess the risks and provide recommendations on how to successfully perform the observation and process the imagery to global surface temperature. The purpose of this paper is to provide highlights of the NESC

assessment study [Ref. 21]. This will include the description of the companion observation and the subsequent analysis of the thermal imagery.

2. Rationale for Thermal Imaging

A Flight Test Objective (FTO) is a technical statement defining an objective to be accomplished during a test flight. A primary FTO of the EFT-1 flight test was the determination of the capsule heat shield and backhell aerothermodynamic environment during reentry (OFT1.091). This type of FTO generally requires quantitative data to be collected to validate a mathematical prediction of subsystem performance and/or environment. Measures of Performance (MOP) are often used to describe the specific types of measurements to be collected. Traditional in-situ Developmental Flight Instrumentation (DFI) installed on the heat shield was to be the primary measurement method to satisfy OFT1.091. However, a secondary MOP specified an observation during reentry through external ground-based or airborne assets with thermal detection capabilities. The NESC's involvement in the EFT-1 observation was initiated from concerns within the NASA Orion Flight Test Management Office (FTMO) that the MOP specifying a quantitative, spatially resolved thermal observation of the EFT-1 capsule during reentry through external ground-based or airborne assets could not be met. Two years prior to the planned 2014 launch of EFT-1, a request was made to the NESC to provide a risk reduction assessment to inform the Orion Multi-Purpose Crew Vehicle (MPCV) Program on the ability to provide global heat shield temperatures derived from engineering quality infrared imagery during the EFT-1 reentry and to offer recommendations to reduce risk with such an observation.

The MOP for external thermal observation was intended to compliment and serve as a risk reduction in the event of anomalous DFI behavior as has been observed during several Shuttle reentries [Refs. 22, 23] or failure to record DFI instrumentation during reentry as had occurred during an early uncrewed Apollo test flight (AS-201) and the Space Shuttle during STS-1, STS-4 and STS-35. The desire to compliment the thermocouple DFI heat shield instrumentation with image-derived temperature inferred from remote infrared observation is a direct result of the complex and challenging process to accurately reconstruct surface temperature from DFI sub-surface thermocouple measurements. The EFT-1 capsule instrumentation to measure temperature consisted of traditional thermocouples (TC) located in the Avcoat heat shield as shown in Figure 2-1. The limited number of thermocouples were embedded into plugs at various depths in the 1.6 inch thick heat shield in order to protect them from the harsh conditions during reentry. Therefore, the thermocouples do not measure *surface* temperature, rather temperature at their embedded location. Surface temperature must therefore be inferred using inverse methods. As discussed in references 24-26, the post processing of the flight TC measurements requires accurate knowledge of the thermal properties of the material in which the sensor is embedded. Uncertainties in the reconstructed surface temperature arise from assumptions in time dependent material properties and depth of the ablative TPS char layer in the vicinity of the sub-surface TC. Surface temperatures derived by the remote-based observations associated with the NESC assessment were offered as a direct and independent method to infer surface temperature and hence verify the fidelity of the reconstruction process to infer surface temperature from a sub-surface measurement.

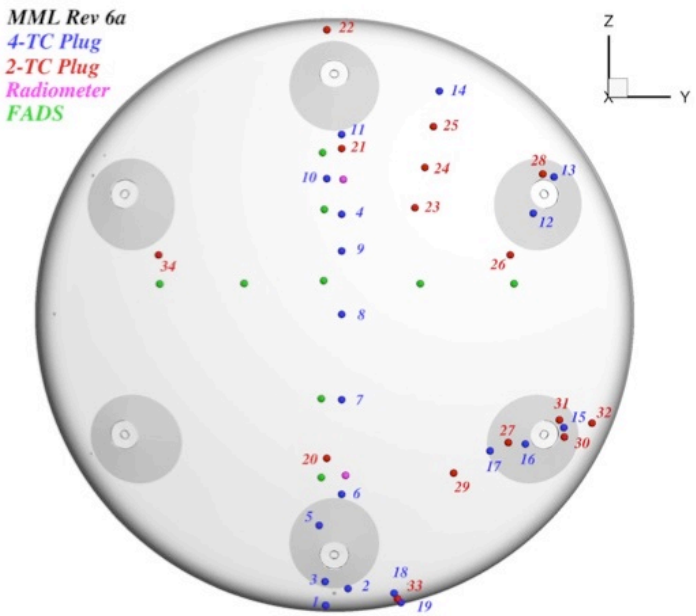

Figure 2-1. Schematic of EFT-1 Heat Shield DFI Instrumentation Layout (subsurface TC locations identified in blue and red)

3. Selection of Measurement Platform

On June 7, 2012, the NESC approved the charter to formulate a team to perform the risk assessment study. The assessment team was derived from a subset of the NASA Scientifically Calibrated In Flight Imagery (SCIFLI) team – a coalition of NASA, United States Navy, Government laboratories, and contractor personnel. At the heart of the assessment was the question of whether or not existing remote thermal sensing capability could provide useful, engineering quality data. To answer this question, an analysis was undertaken to determine where the observation would most likely occur, what type of imaging platform would be required, and if the optical system associated with that platform was capable of providing useful spatial resolution. To perform the analysis, the assessment team leveraged tools developed under NESC assessment 07-048-E [Ref. 1] and successfully utilized by the Space Shuttle Program-sponsored Hypersonic Thermodynamic Infrared Measurement (HYTHIRM) team to provide global thermal images of seven shuttle flights during hypersonic descent (2009-2011) and the Dragon capsule during its inaugural reentry in 2010.

Early trajectories were provided to the assessment team to determine the expected location of peak heating along the anticipated flight path of the EFT-1 Orion capsule during reentry. In contrast to the Space Shuttle, where a 90-min (or 48-hour) delay in returning from low Earth orbit would significantly shift the ground track, the EFT-1 ascent and subsequent reentry ground track was not susceptible to these shifts. That is, for any given launch time, the location of the flight path relative to the Earth remains unchanged. Therefore, the process of determining the general location of the peak heating event relative to any fixed point on Earth was far less complex. The position along the flight path where the EFT-1 capsule experiences maximum heat shield temperature (peak heating) was specified from a fixed point in time; either from capsule separation from the Delta IV upper stage or from Entry Interface (EI) that was designated as an altitude of 400,000 ft. The Virtual Diagnostic Interface (ViDI) [Refs. 27-29] tool developed at NASA Langley Research Center (LaRC) was used to process the 6-degree of freedom trajectory information to visualize the timing of critical events along the entire trajectory on a virtual three-dimensional (3-D) Earth. Recovery of the capsule was to occur approximately 600 nmi off the California coast as shown in Figure 3-1. Peak surface temperature on the heat shield was anticipated to occur a few hundred miles west of the recovery point over the Pacific Ocean - in the absence of any remote land islands capable of providing imaging from the ground.

Sea-based imaging systems, while theoretically capable, inherently possess all the challenges of a ground system along with other concerns such as making an observation through an image degrading marine layer with high aerosol content. In addition, pointing stability requirements at sea represents a significant hardware integration

challenge in terms of gyro-stabilization and isolation from the ship motion and engine vibrations. Therefore, any mobile, or fixed ground or sea-based imaging assets were immediately excluded from further consideration.

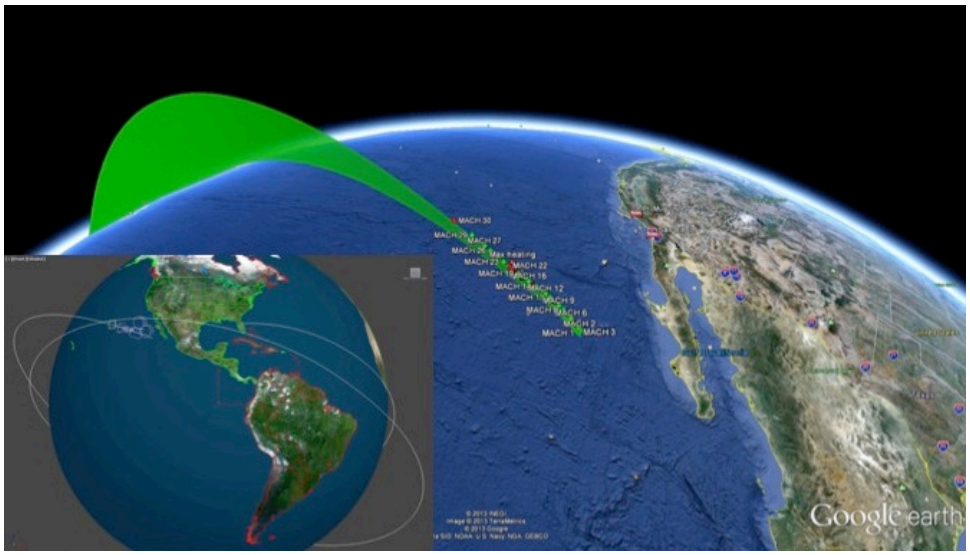

Figure 3-1. EFT-1 Proposed Reentry Flight Path (circa 2013) with Splashdown off the Coast of California

Naturally, imaging strategies over remote bodies of water tend to favor the flexibility and range of airborne systems. Five aerial platforms operated by either the Department of Defense (DoD) or NASA were initially evaluated by the assessment team. Based upon cost, range, endurance/loiter time, and previously demonstrated capability for tracking high speed moving targets, a U.S. Navy NP-3D Orion, Figure 3-2, stationed at the Naval Air Warfare Center, Point Mugu, California was ultimately recommended for further consideration.

Figure 3-2. U.S. Navy NP-3D Cast Glance Aircraft (Call Sign Bloodhound 300)

The optical system on the Navy P-3, often referred to as Cast Glance, is comprised of a set of electro-optical platforms mounted within the pressurized section of the aircraft. A gyro-stabilized gimbaled mirror tracks the target and directs the light towards a fixed telescope rather than moving the camera and lens itself. The gimbaled mirror can be steered manually or assisted through the aid of a computer aided pointing system. Through a series of beam splitters and pick-off mirrors, light is then diverted to several video, digital and high-speed visual, and infrared (IR) imaging sensors. References 8–10 provide a more detailed description of the Cast Glance optical sensor suite. With the ability to stay aloft for approximately 11 hours, the Navy P-3 would only require 2–3 hours of one-way transit time from its home base in California to reach the general area for the desired observation leaving 4–5 hours of loiter time if necessary.

4. Measurement Capability

The next phase of the assessment was directed at determining the optimal aircraft observation location and estimating the expected resolution and radiometric performance of the existing Cast Glance infrared sensors. The Space Shuttle observation campaigns from 2009–2011 resulted in some remarkable thermal imagery yielding global surface temperature maps [Ref. 16] from seven successful IR observations. Relative to the Space Shuttle, the EFT-1 capsule is significantly smaller in size and returning from beyond low earth orbit and as a result, heat shield surface temperatures were expected to be up to a factor of 2 higher during reentry. Given these fundamental differences, it was not clear at the beginning of the assessment if the target (Orion capsule) could be acquired at extreme distances, if sufficient spatial resolution could be achieved at the point of closest approach, or if the higher surface temperatures and the ablative nature of the heat shield TPS would preclude useful surface temperatures derived from the IR imagery. To answer these and other questions, the assessment team utilized a number of simulation tools developed and tailored for use by the assessment team prior to the observation. These simulation tools allowed the team to set expectations with the technical stakeholders and ultimately provide the sensor operators and flight planners with synthetic imagery from which to formulate deployment recommendations, determine pre-flight sensor configuration options, and locate optimal aircraft observation locations. The use of the modeling tools also served as an essential element of risk mitigation.

A. Aircraft Observation Location

The location of the imaging aircraft is driven by a number of factors including (but not limited to) EFT-1 launch time, local weather, sun position, aircraft performance parameters, EFT-1 entry trajectory, and hazard zone boundaries along the flight path. The geometry between the observing aircraft and the target vehicle determines the aircraft maneuvers to maintain the capsule in the field of regard and must satisfy optical system hardware constraints associated with elevation angle and slewing rates. For safety considerations and tracking limitations, the aircraft cannot be located directly under the EFT-1 flight path. Typically, the observing aircraft is positioned offset from the ground track by some predetermined distance. The P-3 standoff distance from the EFT-1 ground track was based upon elevation constraints looking thru the aircraft window and keep-out zones imposed by hazard analysis of a potential capsule break up. The relationship between the EFT-1 ground track, the keep-out zone boundary, and the flight path of the P-3 aircraft is shown in Figure 4-1. Blue points indicate timed locations of the P-3 aircraft as the capsule would approach the point of peak heating.

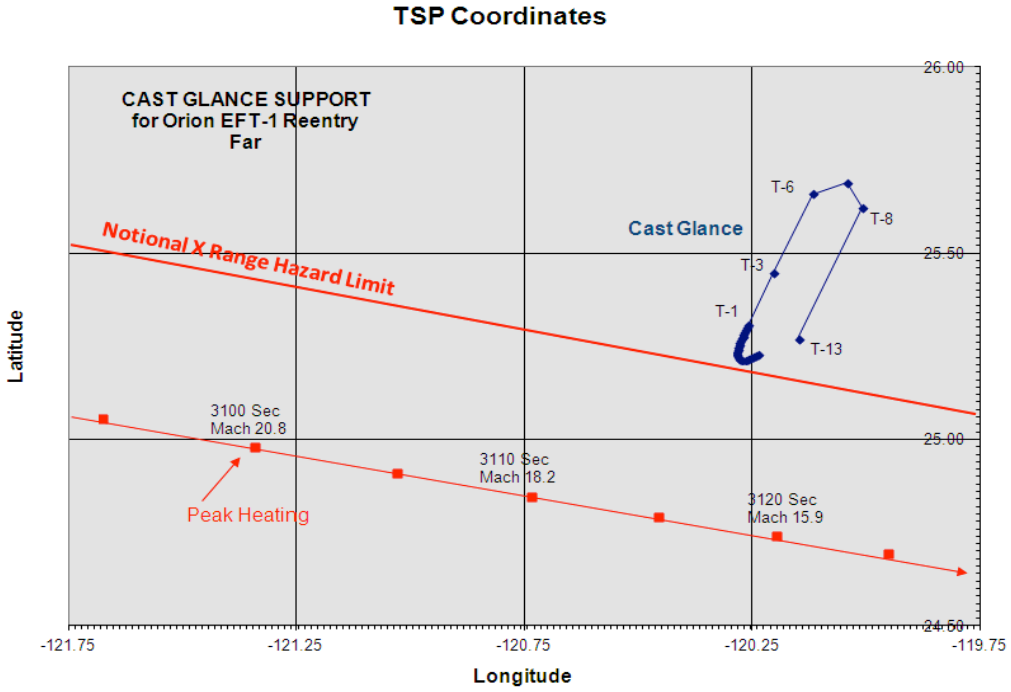

Figure 4-1. EFT-1 Ground Track and Hazard Keep-out Zone

B. Spatial Resolution

Additional information in the form of the Orion capsule surface computer aided design (CAD) definition is imported into the ViDI tool [Refs. 27-29] to ascertain and then graphically display the spatial resolution performance of the imaging system. The ViDI program identifies optical system specifications from an asset database (e.g., a particular telescope mount on an aircraft or a land-based system) and quickly determines the view/orientation of the target based on the asset position and the location of the target during reentry. Information in a preliminary EFT-1 trajectory file, provided in 1-Hz increments, was used in conjunction with the surface CAD of the capsule to create dynamic synthetic imagery in the interactive 3-D virtual environment. A scaled representation of the flight test vehicle was located and orientated at each time step specified in the trajectory file. Entering latitude, longitude, and altitude defined the location for a virtual camera on the P-3 aircraft. Both the virtual camera field of view and the pixel resolution were matched to the performance of the optical system carried on the P-3 aircraft, thus, rendering a pixel-to-pixel accurate simulation of the expected imagery. A simulation of this nature captures the expected spatial characteristics (e.g., viewing perspective, pixels on target), but is not radiometrically accurate.

An example of the ViDI output, Figure 4-2, depicts the expected capsule orientation and spatial resolution from an existing Cast Glance NIR camera as configured for a thermal observation near the expected point of peak heating. Based upon the telescope specifications and the sensor performance and the width of the capsule at a nominal slant range (i.e., distance from capsule to aircraft) of 37 nmi, each pixel associated with the NIR sensor represents approximately 10 inches. Some image degradation from the atmosphere and the optical system, and blurring due to jitter and motion of the aircraft, was expected to decrease the resolution of the unprocessed imagery to 12–15 inches per pixel (advanced image processing techniques can restore some of the spatial resolution lost due to atmospheric effects and or jitter). At the native spatial resolution of 12-15 inches per pixel, thermal features such as boundary layer transition (if present during the observation period) could be readily identified. Localized temperature gradients expected within the six compression pads near the outer edge of the heat shield (Figure 2-1) would not be spatially resolved but the averaged elevated temperature expected in the general vicinity could be detected over several pixels. As such, the estimated spatial resolution and the heat shield viewing perspective obtained with the Cast Glance imaging system positioned for an observation near the peak heating event was acceptable to the engineering community.

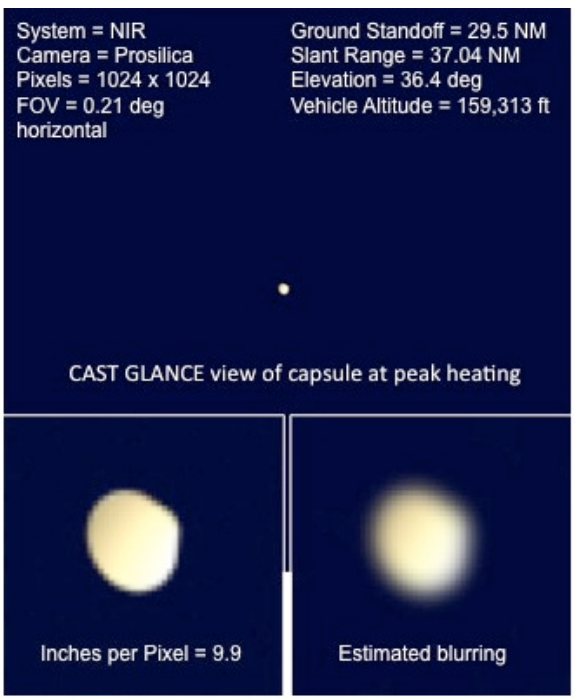

Figure 4-2. EFT-1 Ground Track and Hazard Keep-out Zone

C. Radiometric Considerations

The Orion capsule was a non-cooperative target. That is, real-time positional information was not to be broadcast. Limited telemetered information from the capsule to an orbiting satellite would exhibit large time lags if relayed to

the aircraft. With the general observation location established, the assessment team then sought to determine if the infrared sensors onboard the P-3 aircraft would have sufficient sensitivity to passively acquire and track the capsule at long range. Previous SCIFLI observations of reentry were successful at long-range acquisition because the target's surface temperatures were in excess of 1000 °F providing sufficient signal-to-noise ratio for detection as the vehicle emerged over the hard Earth horizon. If the IR signature of the Orion capsule was too weak and not detectible long-range at low angular velocities, experience has shown it would be more difficult to acquire at higher angular velocities when the capsule approached the vicinity of the aircraft. The assessment team utilized a set of planning tools [Refs. 8, 30-33] to establish processes and make recommendations for reliably acquiring and tracking the EFT-1 capsule during reentry. In contrast to ViDI, these radiometric tool sets quantitatively characterized the optical signature presented by the capsule to IR sensors including the attenuating and image degrading effects of the atmosphere, and ultimately determined the anticipated infrared sensor response.

The optical signature (irradiance) of the capsule was estimated based on the predicted surface temperature provided by computational fluid dynamics. Predicted temperatures on the EFT-1 heat shield during several phases of reentry are shown in Figure 4-3. Time zero in this figure corresponds to the point in time when the capsule is separated from the Delta IV upper stage — with the capsule recovery in the Pacific occurring approximately 1 hour later. From the vantage point of the imaging aircraft, the capsule was expected to appear over the Earth's horizon (at a distance of 1330 nmi) approximately 5 minutes before the capsule reached its maximum surface temperature. To initially locate the capsule, the optical system on the aircraft would be passively staring at a predetermined point in the sky based upon a projected flight path. At the horizon break, the capsule heat shield was expected to be approximately 40 °F (277 K) because the initial line-of-sight view from the aircraft would occur when the capsule was still exoatmospheric (well before the onset of frictional heating from the atmosphere). Just a few minutes later and one minute from passing the location of the observing aircraft, the heat shield temperature was expected to rapidly increase to approximately 1300 °F (977 K). At peak heating, the surface temperature was expected to increase from its baseline temperature by two orders of magnitude, to approximately 4,000 °F (2,477 K). At these substantially higher temperatures, the capsule irradiance would peak in the near infrared (NIR) waveband and an NIR sensor would likely be targeted for the desired spatially resolved thermal measurement.

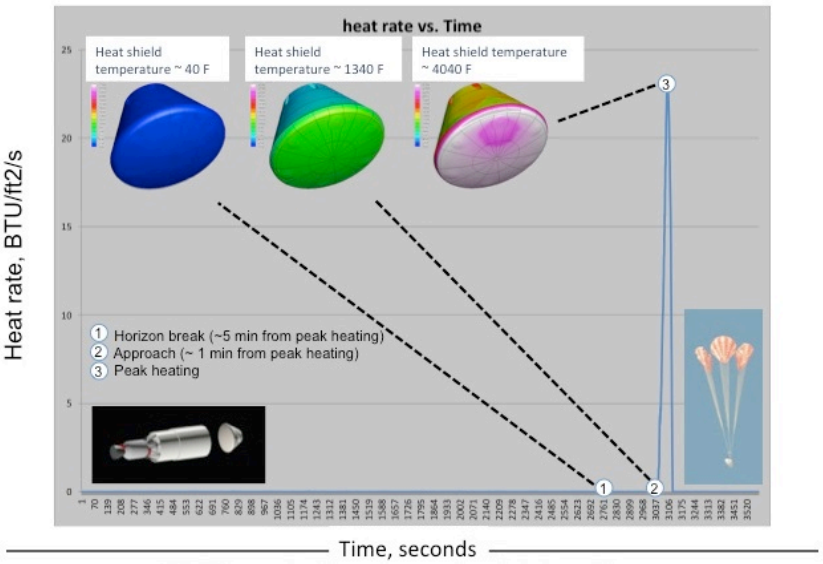

Figure 4-3. Predicted Surface Temperatures on the EFT-1 capsule During Several Phases of Reentry

During a Space Shuttle observation using the same Navy aircraft, the high temperature windward surface of the vehicle at approximately 1,500 °F (1,089 K) presented a strong photon-rich emission in the NIR waveband as it emerged over the horizon. So an NIR sensor could be effectively utilized for both long-range acquisition and thermal imaging at the point of closest approach. When it was subsequently determined the Orion capsule heat shield would have a surface temperature an order of magnitude lower than the Space Shuttle Orbiter at horizon break, it was concluded that the capsule would be very difficult to distinguish from the sky background using the Cast Glance NIR sensor. It was logically assumed that sufficient signal strength would appear in the more photon-rich mid wave infrared (MWIR) waveband for acquisition and tracking purposes when the capsule was at extreme

distance, spatially unresolved (i.e., a point source), and at low temperature. However, subsequent discussions with the MPCV program revealed that to control the heat shield thermal environment while in orbit, the Avcoat surface would be painted with a white epoxy enamel paint and covered by a thin aluminized Kapton® film. While these materials would quickly ablate after atmospheric entry interface, it would still be present during the long-range acquisition from the aircraft. Surface optical testing of several Avcoat samples to determine emissivity [Ref. 21] revealed that the metallic tape actually attenuated IR signatures in the MWIR. Additional radiometric analysis later showed that during the long-range acquisition phase when the aluminized tape was still in place and highly reflective, the irradiance from the capsule would be dominated, particularly in the short wave infrared (SWIR) waveband, by solar reflectance and not thermal emission. This solar irradiance, which is result of a favorable sun/capsule orientation, would further enhance the signal-to-sky background thereby increasing the probability of "seeing" the capsule at long range. To reduce risk, a long-range acquisition strategy centered about the Cast Glance SWIR sensor was recommended to provide a better opportunity to distinguish the relatively dim capsule from the sky background.

During the period of maximum heating and spatial resolution, analysis revealed the NIR system would have no shortage of photons available, and either the use of a neutral density filter or reduced camera integration times would be required to avoid saturation of the infrared detector. Figure 4-4 provides an example of the radiance model output. On the left, the capsule irradiance estimated to reach the NIR focal plane array using a filter and an exposure time of 20 msec is displayed graphically. The corresponding image of what the sensor operator would observe on his tracking display (intensity/counts) is shown on the right. The estimates assume some blurring due to the atmosphere and aircraft motion. At a range of approximately 48 nmi, the capsule is spatially resolved. Estimated pixel resolution in these radiometrically accurate synthetic images was consistent with earlier ViDI results.

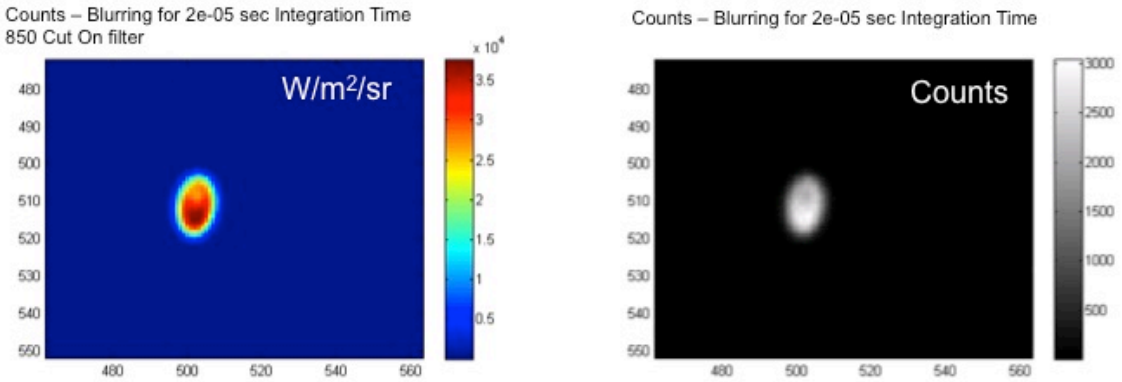

Figure 4-4. Predicted Irradiance in the NIR Waveband at the Time of Peak Heating. Distance to Capsule = 48 nmi. Elevation Angle = 27 deg. 850 mm Cut-on Filter.

For the accurate capsule heat shield temperature determination as inferred from IR intensity measurements, accurate book keeping of the photons collected at the detector focal plane array must be performed. Surface temperature is inferred from the photons emitted from the heat shield by virtue of its temperature. However, there are other sources (and attenuators) of photons that must be identified and potentially accounted for. One of these irradiance sources is from the high-temperature shock layer between the heat shield and the observing aircraft. Heat shield ablation material can represent both an irradiance source as well as a potential attenuator of the infrared radiation emanating from the heat shield.

To ascertain the potential attenuation of the heat shield irradiance from the presence of ablation products (or additional emissions from ablation particulates) in the wavebands of interest, a supplementary analysis was performed. Two radiation transport tools were exercised to assess the levels of expected emission in the NIR: These two codes were the Standard Plume Ultraviolet Radiation Code (SPURC) [Ref. 34], and Nonequilibrium Air Radiation Code (NEQAIR) [Ref. 35]. Near surface flowfield properties provided by computational prediction near the point of peak heating were used as inputs to these two codes. SPURC was originally developed to provide rocket exhaust plume signatures (ultra-violet through LWIR) and includes both gaseous emission and particulate (soot, alumina, etc.) scattering / emission. However, the gaseous emission uses band models and does not accurately address non-equilibrium conditions experienced at very high temperatures. NEQAIR computes radiation in the same part of the spectrum but uses line-by-line methods instead of band models for temperatures approaching

17,500 °F (9,978 K). NEQAIR is specifically tailored for assessing hypersonic shock layer radiation but does not address particulate emissions.

To begin, an estimate of the boundary layer edge properties and chemical species was obtained from the MPCV Aerosciences team. The chemical composition provided was from an equilibrium calculation using Avcoat™ ablation products mixed and reacted with boundary layer air species at representative boundary layer conditions. A simplified problem was constructed to investigate the effects of this layer on the NIR measurements. A homogenous slab of gas was assumed with the species concentrations provided at the edge pressure over a range of representative temperatures. The thickness of the slab was chosen to be slightly larger than three times the maximum momentum thickness to ensure that the extent of the ablation products into the flowfield would be captured. The results from SPURC and NEQAIR are shown in Figures 4-5 and 4-6, respectively. A range of heat shield surface temperature and shock layer temperatures are presented and encompass the expected conditions during EFT-1 reentry.

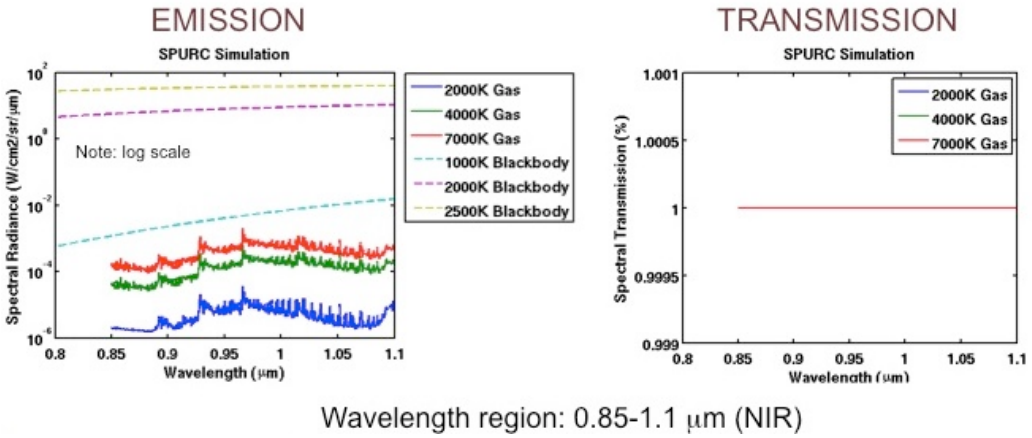

Figure 4-5. Predicted Emission and Transmission from SPURC for a range of Surface and Shock Layer Temperatures

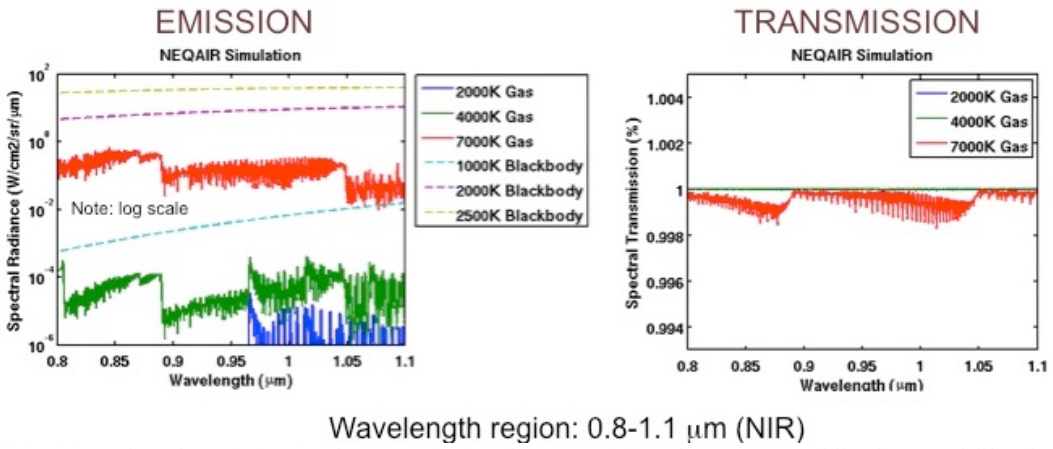

Figure 4-6. Predicted Emission and Transmission from NEQAIR for a range of Surface and Shock Layer Temperatures

The predicted emission data from both codes (left plots) compare the magnitude of the NIR emissions from the heat shield surface relative to those from the high-temperature gas in the shock layer. Note a log scale was used due to the large differences in magnitude between the two photon sources. The SPURC emission predictions (Figure 4-5) indicate that the photons from the heat shield by virtue of its temperature are dominant. Increases in NIR emissions from the presence of water vapor in the shock layer are predicted with SPURC. For a gas temperature of 12,140 °F (7,000 K), the companion NEQAIR results (Figure 4-6) indicated a significant increase in NIR emissions from N_2 (1+) that was not captured by SPURC. However, the emission level is still approximately an order of magnitude less than those from the heat shield at a surface temperature of 3,150 °F (2,000 K). The conclusion is that while the

radiative heating from the shock is not negligible, the NIR radiation from the high-temperature heat shield would dominate that emanating from the shock layer.

The transmission data from these two codes (right plots) suggests little to no absorption of the head shield emissions in the NIR waveband within the high temperature shock layer. A value of unity indicates the emissions leaving the heat shield surface are transmitted through the high-temperature gas cap with no loss. The NEQAIR results, Figure 4-6, indicate a slight absorption in the NIR waveband for the higher-temperature gas that the SPURC (Figure 4-5) does not capture but it is very small in magnitude.

The final outcome of the ablation study determined that while the shock layer radiation needed to be accounted for during the period of peak heating, the correction would be only on the order of three percent. This would be accounted for in the post-flight data processing, and would not alter the method of data acquisition. Ultimately, the Cast Glance aircraft had to position itself far down the trajectory from the peak heating location due to weather constraints at the originally planned Test Support Position. The imagery was acquired when the Orion capsule wasat approximately Mach 10 instead of the planned Mach 21. Under these conditions the shock layer radiation and ablation of the heat shield were minimal, and corrective factors were not applied for the final data processing.

The NESC assessment study thus far had shown not only a quantitative observation was possible, but that the risks inherent to the unique aspects of this flight test (e.g., ablator heatshield) were well understood and could be mitigated. The results were presented to the NESC Review Board and the authority to proceed toward an actual observation granted.

5. Simulation & Training

Upon approval of an EFT-1 thermal observation campaign, a wide array of activities began to prepare for the scientific, logistic, hardware, software, and human aspects of the observation. These activities and associated procedures have evolved over 17 observations spanning more than 10 years under Hypersonic Thermodynamic Infrared Measurements (HYTHIRM) and later SCIFLI. Coordination of a remote observation associated with a high-speed target is a dynamic logistical effort that requires the gathering, analysis, and dissemination of time-critical information. To assure critical information is developed, received, and distributed to the appropriate team member at the proper time, a Mission Execution Plan (MEP) was created. The MEP is a comprehensive document encompassing a wide range of reference information tailored to specific events and requirements for coordination of an observation campaign. The EFT-1 MEP identified the roles and responsibilities of the operations team, described processes and procedures for conducting the observation, identified training opportunities and the noted the delivery of any critical items such as hardware, software, and trajectory information. A companion day of launch schedule identified critical events during the EFT-1 flight test and provided a minute by minute checklist as a guide for the EFT-1 operations team.

Mission simulation was a key risk mitigation and a series of Agency-level simulations were conducted for training and proficiency purposes. The assessment operations team was more closely integrated into the flight operations for EFT-1 than in any previous imaging mission, with the status of the observation aircraft being relayed to the EFT-1 Launch Director, the NASA Recovery Coordinator, and the U.S. Navy recovery forces. In mid November, several weeks before the EFT-1 launch, a fully integrated training exercise was held at NASA JSC. To support the training exercises as well as the actual mission, the NESC assessment operations team was provided console space at the Imagery Payload Operations Center (IPOC). The IPOC provided the required communications and workspace in a central location, contributing to the ability to successfully coordinate the EFT-1 observation. The room contained numerous computer terminals, television monitors, landline phones, and counter space. In addition, each console had access to the digital voice intercommunications equipment audio distribution system used to communicate with elements of the EFT-1 Flight Operations team as necessary.

The assessment mission operations team entered this final Agency training exercise with a series of mature procedures and documents including the MEP. During this simulation, the assessment team did not directly receive any green “anomaly” cards, and the Orion capsule largely remained on course and on time for a recovery off the California coast. While in orbit, an anomaly associated with the DFI batteries was identified. The assessment team technical lead participating in the exercise suggested the possibility of repositioning the P-3 peak heating aircraft in the event of battery failure and loss of DFI instrumentation. The battery issue was resolved and the P-3 remained at its designated observation location. The real-time simulation, which began at T-minus 6 hours and continued past

splashdown, resulted in a 12-hour exercise that solidified the mission planning, reinforced communication protocols and provided confidence for the actual mission operations.

6. Collection of Thermal Imagery

This section of the paper describes the general chronology of a few major events leading up to and including the thermal observation campaign conducted by the NESC assessment mission operations team. In early November of 2014, a delta Critical Mission Review (CMR) was held to review risks and status the readiness of the assessment team to proceed with the observation campaign. The participants included representatives from NASA JSC, assessment stakeholders, the NESC, and the aircraft flight crew/sensor operator. No outstanding hardware and software issues were identified. A review of sensor configuration recommendations based upon JHU-APL radiance modeling was made and no changes were identified or expected. The risk associated with a P-3 aircraft schedule conflict was re-evaluated and characterized as low. At the conclusion of the delta CMR, the team was polled and it was determined that deployment to JSC for missions operations would commence on November 30. The operations team arrived at NASA JSC several days in advance of the planned December 4th launch to configure their console stations in the IPOC. A photograph of the assessment operations team at their IPOC duty stations is shown in Figure 6-1. Live weather updates and EFT-1 flight information were fed to the display monitors.

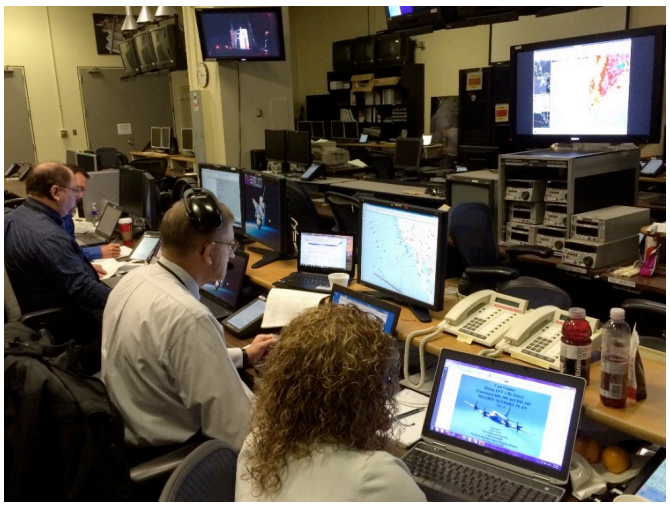

Figure 6-1. Assessment Mission Operations Team on Console at the NASA JSC IPOC for the EFT-1 Observation

December 1, 2014: Three days before a scheduled December 4 EFT-1 launch the mission operations team assembled in IPOC for the dress rehearsal flight with the Navy aircraft. This risk mitigation flight provided the flight crew and sensor operators time to synchronize and fine-tune their proficiency. The P-3 observation aircraft, shown in Figure 3-2, departed from its home base in California after an EFT-1 "launch confirmation" during a mock countdown. During the transit flight, the operations team at NASA JSC coordinated high frequency radio communication with the aircraft using its designated military call sign, BH-300. All backup forms of communication (e.g., Iridium SatPhone, Global Positioning System tracker) were successfully demonstrated. The P-3 crew practiced their racetrack patterns to be flown during the actual observation, working to position the aircraft at the desired location at the precise moment in time that the capsule would encounter EI. The exercises went smoothly, and the P-3 had an uneventful return to base.

Later that evening, sensor calibrations were performed on BH-300's infrared sensors at Point Mugu Naval Air Station. The calibration was moved up a day from its originally scheduled time as adverse weather was predicted to move into the area. Evening calibrations were desired to minimize the effects of solar illumination and scattering from particulates suspended in the atmosphere. To calibrate the IR systems, two blackbodies were setup at a convenient location on the tarmac approximately 500 ft from the Cast Glance aircraft observation window. The blackbody set point temperature were representative of those expected on the EFT-1 heat shield during reentry. A calibration data set consisted of IR intensity data collected over the range of anticipated sensor integration (exposure) times at each temperature set point. A full and detailed description of the calibration data collection

process, the hardware used, and the subsequent analysis to convert measured IR intensity counts to in-band radiance values and ultimately to temperature is documented in ref. 21.

The long-range weather forecasts for the day of EFT-1 launch at the aircraft departure location and the observation location off the coast of San Diego began to converge and suggested clouds at the planned observation location to view the heatshield near Mach 20 could become problematic. Weather conditions were expected to continue to be dynamic over the next few days.

December 2, 2014: Two days before a scheduled December 4 EFT-1 launch, a flight readiness review was held with the Navy. In this briefing, the health of the aircraft systems were discussed, the status of the launch was provided and the science/engineering objectives were reviewed with the crew/sensor operators. Hazard zone boundaries and protocols pertaining to a capsule break up or an abnormal propulsive burn of the Delta IV upper stage just prior to capsule separation were reviewed. BH-300 was "go" to provide imagery support.

Launch weather at the Cape continued to look favorable with concerns noted that ground winds at EFT-1 lift off and ascent through precipitation could become an issue. Forecasted local weather at the planned observation location in the Pacific indicated favorable viewing with scattered broken clouds below the nominal 25-kft operating altitude of BH-300. At this point in time (two days before launch), weather forecasting tools suggested very unfavorable viewing conditions at the peak heating observation location should the launch slip by 24 hours. As such, the operations team began discussions of alternate locations for thermal imaging.

December 3, 2014: One day before a scheduled December 4 EFT-1 launch, the operations team and flight crew observed a mandated day of rest. Communication between the operation team and the squadron was minimal. No additional information regarding trajectory updates was anticipated or received.

The weather prognosis for a Thursday launch at the Cape remained acceptable and observation conditions at the planned peak heating location continued to look very favorable. If the EFT-1 launch was unsuccessful on Thursday morning, the forecast for Friday at the peak heating observation area at the time of the recovery window called for a significant increase in the presence of high, thick obscuring clouds.

December 4, 2014: As per pre-defined timelines, a majority of the assessment mission operations team arrived on console in IPOC at 2:30 am Central Daylight Time (CDT). Sleep shifting was required by select team members to support post-imaging operations (data transfer, etc.) in the event the observation was successful. The entire team was in place several hours before the scheduled launch window opened at 6:05 am CDT. As per mission timelines, the aircraft crew was periodically provided updates on weather along their expected transit route and at the observation location.

Mechanical issues associated with a fuel valve on the Delta IV ultimately led to a launch scrub with a 24-hour recycle to another attempt. Had a launch occurred, the local weather at the desired peak heating observation location would have been ideal with no significant high-altitude cirrus clouds to interfere with the observation. The remainder of the day was spent monitoring the predicted weather at the Cape, the staging locations for the aircraft and the planned observation sites for the next launch attempt. Unfortunately, the prognosis for a clear line of site for thermal imaging on Friday, December 5, was poor.

December 5, 2014: The hardware issue associated with a valve on the Delta IV booster was resolved over night and the decision to proceed towards launch was made by the Launch Flight Director. The operations team located in the IPOC was in place several hours before the scheduled launch window that opened at 6:05 am CDT. As expected, the prognosis for acceptable viewing weather at the desired thermal observation location was poor. Periodic updates weather sources reconfirmed the forecast as the launch count preceded forward. Because significant cloud coverage was expected at the planned observation site, satellite information was used to determine possible alternate imaging positions that would present a cloud free line of sight (CFLOS) to the capsule. A CFLOS software package developed by Johns Hopkins University Applied Physics Laboratory, infers cloud tops and bases from real time satellite measurements and indicates the level of obstruction by clouds along the line of sight from the observer to the target. Figure 6-3 provides a graphic-based CFLOS forecast for viewing conditions at the peak heating observation location (designated #1) off the coast of Baja California. In Figure 6-3, the colors signify the percentage within any particular cell (~30x30 nmi) that clouds will prevent a line of site from the P-3 to the capsule when looking up from 25,000 ft. Poor, if not impossible, viewing conditions were expected at the desired thermal observation location (#1) with potentially more acceptable viewing conditions further east near the edge of the forecast cloud bank (#2).

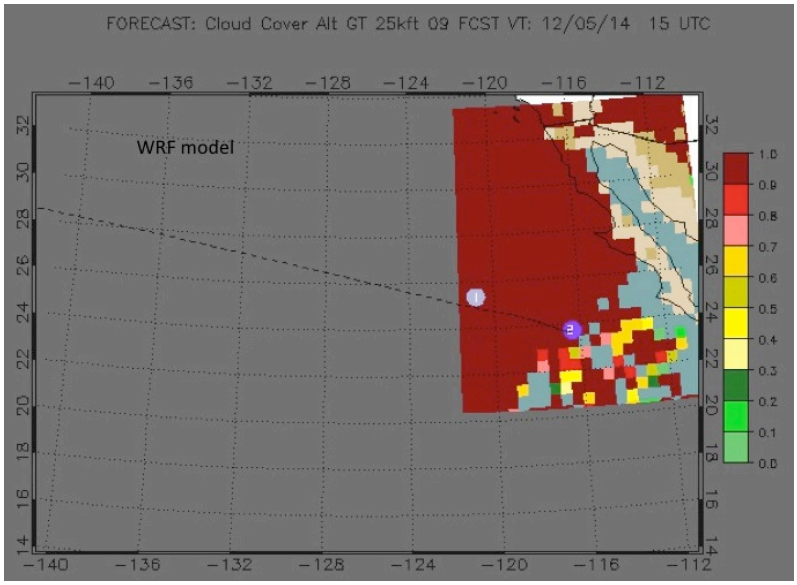

Figure 6-3. Forecasted Cloud Free Line of Sight for Observer Looking up From 25,000 ft

The EFT-1 countdown entered its terminal phase with no issues encountered and liftoff occurred at the designated time at the beginning of the launch window. With a successful launch confirmation, the imaging aircraft departed and proceeded to its designated observation location (#1) to begin scouting the local weather conditions. BH-300 arrived at its designated observation location approximately 2.25 hours prior to EFT-1 reentry. As anticipated, the aircraft crew reported solid overcast conditions at their desired observation location and per contingency plans, the aircraft began transiting east towards the recovery zone along the EFT-1 ground track searching for a favorable imaging location.

As the capsule rapidly approached atmospheric entry interface, a small area with acceptable viewing was located approximately 180 nmi downrange of the originally planned observation location. With the capsule just a few minutes away from view, the flight crew immediately began to enter into an ad hoc timing pattern to position the optical systems for an observation. This unrehearsed response was only possible because of the crew's skill and expertise, and familiarity with the planned sequence of events. Shortly thereafter, the crew reported that the capsule had been successfully acquired and its sensor operators were actively tracking with the high spatial resolution NIR detector. Analysis would later reveal the infrared imagery had been acquired for approximately 63 seconds when the capsule was decelerating from approximately Mach 13 to Mach 6. The relative location of the EFT-1 capsule flight path, the originally planned observation location for peak heating at Mach 20 and the repositioned location of BH-300 is shown in Figure 6-4. The imaging aircraft was stationed at an altitude of approximately 33,000 ft during the observation as the capsule was descending thru an altitude range of approximately 141,000-134,500 ft. Based upon time synchronized navigational data from both vehicles, the aircraft and its crew observing the capsule were separated by approximately 40 nmi. As the capsule passed by the aircraft, it was momentarily lost in a cloud bank. The capsule was subsequently reacquired, tracked and observed at extreme range for an additional 195 seconds through parachute deployment at subsonic Mach numbers.

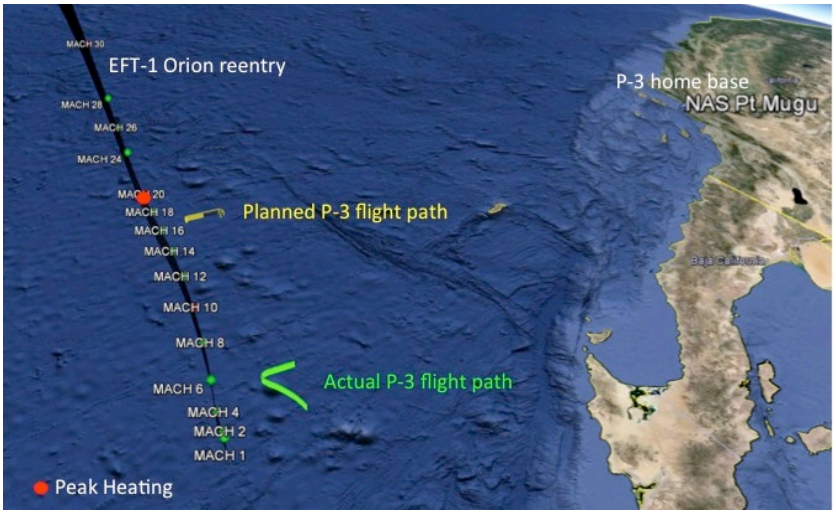

Figure 6-4. EFT-1 Capsule Reentry Track and Flight Path of the BH-300 Observation Aircraft (Planned, Yellow; Actual, Green)

7. Image Processing to Global Temperature

Pre-flight knowledge of the capsule's expected irradiance was extremely beneficial to the detector operators who, in real time, were able to adjust the infrared sensor integration times manually to assure that the raw intensity imagery was collected in a manner that spanned the sensor's maximum dynamic range, while mitigating against saturation. The initial assessment from the image analysis team led by JHU-APL concluded the operator had managed the sensor configuration effectively during the observation, and that after the initial acquisition, little to no saturation existed in the individual frames of thermal imagery. During the 63 sec observation, approximately 900 unsaturated NIR images were identified and evaluated by the analysts at JHU-APL. Many "clear" frames free of significant blurring and distortion were found and the thermal footprint of the six individual compression pads on the EFT-1 heat shield was distinctly visible. The ability to resolve these features was a testament to the fidelity of the preflight visual and radiance modeling tools.

The process of providing a subset of quality global temperature images of the heat shield from these 900 raw (un-saturated) near infrared intensity images is provided in detail by Spisz [Ref. 36]. First, there must be no indication of clouds in the line-of-sight. Intensity from the mid-wave infrared sensor, which is sensitive to water vapor and has a wider field of view, is reviewed to identify abrupt temporal changes in both the capsule and foreground intensity indicative of a thin cloud. Second, individual imagery frames that display detrimental blurring effects due to relative motion (i.e, sensor and capsule), vibration (i.e., jitter), and atmospherics (i.e., local pockets of density variations) are removed. Third, imagery frames near times when the reaction control system (RCS) thrusters are firing are then eliminated. Figure 7-1 provides a sample sequence of cropped views based on the full frame native (unprocessed) near infrared intensity imagery. The Mach number and slant range estimates shown in this figure were based on an EFT-1 pre-flight trajectory and not the as-flown trajectory. This is because the as-flown trajectory took several months to be processed and released to the image analysis team. Note the distinct bright areas on the heat shield periphery correspond to the compression pads. Lastly, image frames near the end of the observation period, when the viewing geometry of the heat shield was becoming too oblique (frame 8787 and greater, Fig. 7-1), were also eliminated.

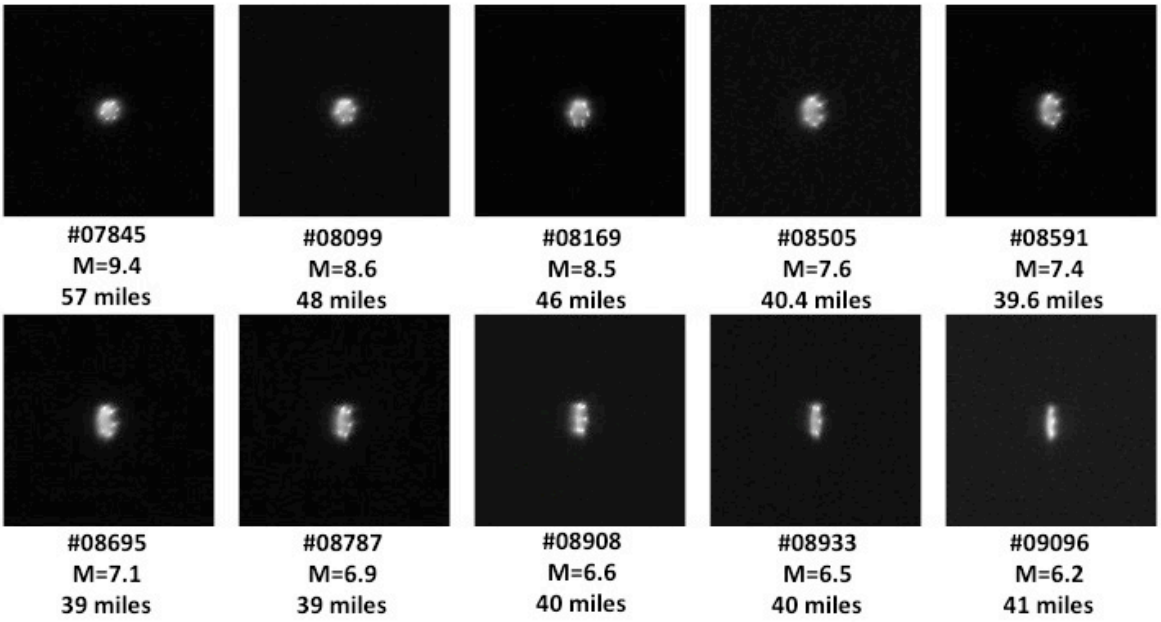

Figure 7-1. Sequence of Raw (Native) NIR Intensity Images Showing Perspective Change of Heat Shield as Capsule Approached the Aircraft

Based upon these collective constraints, five specific times during the EFT-1 reentry were identified at which the corresponding intensity image would be converted to engineering units (temperature). Centered about each of the five selected times during reentry, up to 5 additional neighboring frames are then identified to improve image quality. As discussed by Spisz, interpolation techniques are first used to "over-resolve" and effectively increase the spatial resolution of these neighboring images. The over-resolved frames are then co-registered and averaged to produce a single well enhanced intensity image with increased spatial resolution and improved signal to noise while preserving overall radiometric integrity of the data. A calibration curve is then used to convert image pixel counts to a radiance image for the mission specified integration time. The heat shield irradiance (which is the ultimate goal) was measured at the IR sensor's focal plane array after propagating thru miles of atmosphere to the imaging system optics. Along the line-of-sight path from the capsule to the sensor, the received light incurs atmospheric transmission loss due to scattering and absorption. To infer the desired heat shield irradiance, the image irradiance must be corrected for atmospheric path transmission, solar scattering from aerosols, and path radiance using MODTRAN [Ref. 32] atmospheric modeling. The final step is to convert the heat shield irradiance to temperature by using Planck's black body radiation law and a single in-band emissivity value that was based upon measured values for charred/ablated Avcoat. A more complete outline and detailed discussion on the image processing steps calibration results, atmospheric compensation methods and conversion to surface temperature is presented in refs. 8, 12,17, 21, 36. Table 7-1 shows the resulting 2-dimensional temperature images for the five selected time segments along with a few parameters of interest based upon the as flown EFT-1 trajectory and aircraft flight information.

Image Frame Number:	7848	8028	8251	8474	8632
Image Frame Time Reference (GMT):	16:21:29.9917	16:21:35.9798	16:21:43.3983	16:21:50.8271	16:21:56.0939
Mach number:	9.91	9.33	8.66	8.04	7.63
Target Range (nmi):	65.1	57.2	49.2	43.3	40.6
Target elevation (deg):	15.4	17.4	20.2	22.7	24.1
Raw Image Pixel Footprint (inches):	17.1	15.0	12.9	11.4	10.7
Capsule apparent pitch (angle of attack;deg):	-19.1	-19.1	-19.2	-19.4	-19.4
Capsule "up" (reference to z-axis; deg):	18	18	18	-7	-9
Capsule bank angle (deg):	30.39	22.21	27.85	38.48	46.46
Angle of l.o.s. to heatshield normal(deg):	11.5	33.5	36.0	44.0	53.0
Peak temperature (deg F):	1940	1843	1760	1718	1643
Minimum temperature (deg F):	~1720	~1630	~1520	~1480	~1400
Temperature (deg F): 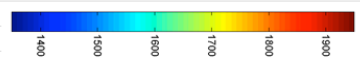	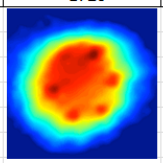	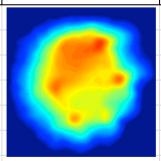	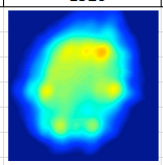	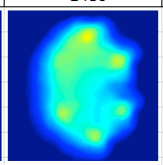	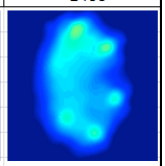

Table 7-1. Final Global Temperature Images for Five Selected Times During EFT-1 Hypersonic Reentry

The final 2-D temperature mappings were a result of the image enhancement and radiometric processes presented in the preceding sections, and most of the inherent data provided as input to these processes have corresponding uncertainties. There are four sources of the uncertainties: sensor noise (i.e., measurement noise), radiometric calibration, heat shield surface emissivity, and atmospheric transmittance.

Because of the image enhancement process where multiple unsaturated frames were registered, co-added, and then averaged, noise statistics were estimated to contribute to approximately 6 °F, based on estimates from prior work [Refs. 12, 17]. The NIR sensor radiometric calibration was very linear, consistent with previous calibration characteristics resulting in an estimated uncertainty of ~2 °F. The emissivity estimate uncertainty is more difficult to quantify because of the unknowns regarding the Avcoat™ surface condition during the reentry. Surface optical testing [Ref. 21] to determine the emissivity of Avcoat TPS samples charred and ablated in an arc jet was made prior to the observation. The measurements indicated a consistent spectral emissivity value of 0.9 in the waveband of interest (near infrared) for viewing angles up to about 50 deg. A conservative uncertainty estimate associated with a 10% decrease in emissivity would account for a temperature increase of approximately 20 °F. Lastly, the atmospheric transmittance uncertainty is difficult to determine because the conditions during the observation were not measured, but interpolated from limited satellite information where the reentry occurred. However, at the aircraft and capsule altitudes, the transmittance was consistent at approximately 0.96%, and typically does not change more than a few percent. A transmittance uncertainty of 5% was assumed and would account for a temperature error of approximately 10 °F (an unrealistic 10% error on the transmittance value would increase the error to ~20 °F). To assess a total uncertainty, each of these sources was combined in quadrature. The total uncertainty for the EFT-1 heat shield temperatures was estimated to be ±15 °F. This is consistent with prior uncertainty estimates for airborne data collections described in earlier work [Refs. 9, 12].

8. Observation Highlights

The imagery-based surface temperatures shown in Table 7-1 are presented on the same temperature scale, indicating the rapid heat shield cooling (i.e., ~300 °F in 36 sec) during the observation. During the period of the observation, the capsule was rapidly decelerating with a small amount of roll as measured by the on-board capsule instrumentation. As planned, the viewing geometry was nearly head-on for the first image shown (i.e., frame 7848) and became more side-on as the observation progressed. In the sequence of views presented in Table 7-1, the capsule roll dynamic can be inferred from the small changes in the compression pad position. The capsule was flying with the hotter area of the heat shield (i.e., the flow stagnation point) at approximately the 11-o'clock position with an angle of attack of ~19 deg.

A process of mapping a two-dimensional (2-D) temperature map to a 3-D surface as was done for previous Space Shuttle observations [Ref. 13] was not attempted with the EFT-1 temperature maps. The accuracy of the iterative

numerical technique developed for the Shuttle thermal imagery was dependent on vehicle edge definition and the presence of distinct thermal features. While the pixel resolution between the Shuttle and EFT-1 thermal imagery is reasonably close, the larger size of the Orbiter vehicle and the presence of sharp thermal gradients in the 2-D orbiter temperature maps readily facilitated the 3-D mapping process.

The footprint associated with the EFT-1 compression pads are very evident but unresolved, because the compression pads are smaller than the pixel footprint in these images. However, if the footprint is the result of localized heating from the posts (and not due to local emissivity changes), then the temperature differences between the compression pad and their immediate surroundings would be in excess of 100 °F.

Consultation with the MPCV Aerosciences team indicated the acreage surface temperatures inferred from the IR imagery were consistent with that inferred from a laminar-based CFD prediction. At no time during the observation when the heat shield was in view (i.e., Mach 9.9 to Mach 7.6) did the thermal imagery indicate the presence of wedge-like thermal footprints associated with hypersonic boundary layer transition as have been observed on the Shuttle [Ref. 16]. Based upon initial expectations of when hypersonic boundary layer transition was expected to occur on the EFT-1 heat shield during reentry (~Mach 20), a laminar boundary layer this late in the reentry was not expected. In practice, the onset of hypersonic boundary layer transition is difficult to predict and when additional factors (e.g., discrete and distributed surface roughness and mass addition/blowing from ablation) are present, it is clear that simple engineering methods lack the sophistication to accurately predict when transition will occur. Based upon circumstantial evidence, it is suggested that it is possible that the boundary layer initially became unstable (i.e., non-laminar) at higher Mach numbers when the heat shield was not under observation. During this time, the wedge patterns would have been imprinted on the heat shield surface. Soon thereafter, it is hypothesized that the boundary layer relaminarized as observed during the observation period. After the heat shield was no longer visible to the Cast Glance IR sensors at lower Mach numbers, the boundary layer would have at some point in time transitioned to a fully developed turbulent state under this scenario.

A heat shield post-recovery image (Figure 8-1) suggests this scenario as plausible by revealing what appear to be multiple wedge-like features emanating from the flow stagnation region. The wedge angles of these features are consistent with the spreading angle of flow turbulence at high hypersonic Mach number. The thermal image obtained at Mach 9.9 (Figure 8-1 inset) has been rotated to align with the stagnation region shown in the heat shield image. If these wedges were produced by elevated heating from flow turbulence, then transition (or non-laminar flow) preceding transition onset had occurred at high Mach number with the flow subsequently returning to a laminar state and the residual heating footprint washed out during the observation time. Alternatively, the transition occurred at supersonic Mach numbers (i.e., less than Mach 7.6) after the observation. However, it is doubtful these wedge-like features would have been imprinted into the heat shield at the temperatures found at these lower Mach numbers.

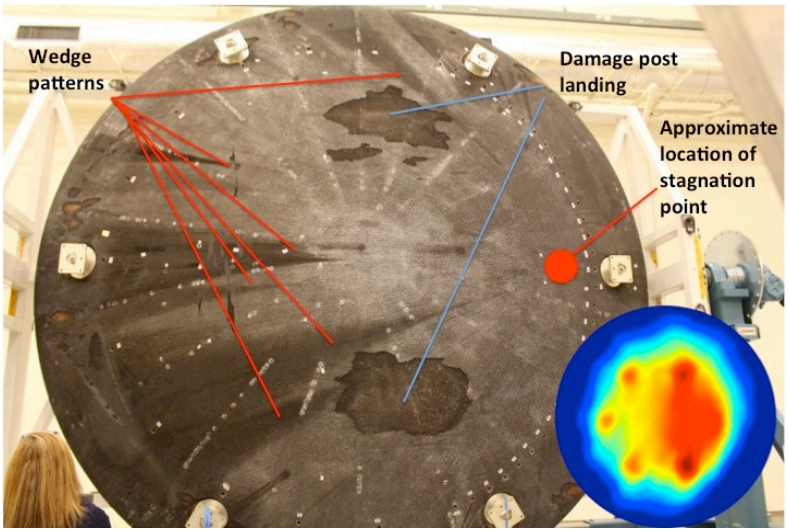

Figure 8-1. Comparison of Global Temperature Image with Post-Flight Image of the EFT-1 Heat Shield

9. Comparison of Thermocouple Data to Image Derived Temperature

Instrumented plugs were installed at multiple points on the Avcoat™ heat shield to measure the sub-surface temperatures during the EFT-1 entry. The plugs consisted of two Type-S TCs, two Type-K TCs, and a Hollow aErothermal Ablation and Temperature (HEAT) recession sensor [Ref. 37]. The Type-S TC nearest the surface was installed nominally 0.1 inch below the surface with the remaining TCs installed at progressively deeper locations. Reconstruction of Avcoat™ surface temperatures using the near-surface TC measurements were performed using the inverse heat transfer capabilities of the Charring Ablator Response (CHAR) code and the design Avcoat™ response model [Refs. 38, 39].

Two EFT-1 heat shield TC locations were used for comparative purposes. These sensors (i.e., plug06 and plug08 – see Figure 2-1) were selected based on their time trace quality (e.g., largely free of apparent non-physical temperature readings observed in several of the near surface EFT-1 TCs), exhibited a relatively smooth monotonically decreasing temperature with time, and were not located near a large temperature gradient. Based on the TC locations, the corresponding locations in the imagery were estimated by using the pixel size references (the "interpolated" imagery in this figure was less than 2 inches/pixel). An example of temperatures extracted along the 2-D surface temperature map associated with the thermal image obtained at Mach 9.9 is shown in Figure 9-1.

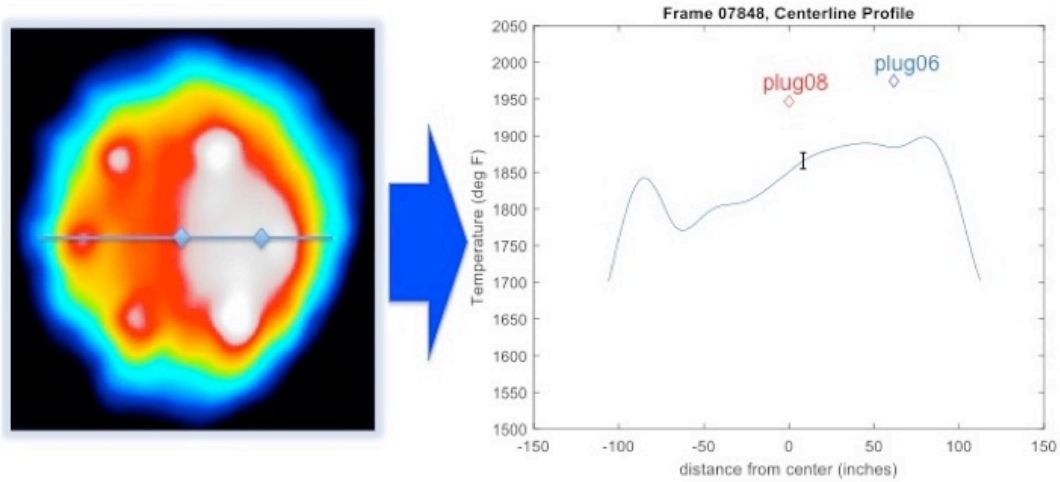

Figure 9-1. Comparison of Image Derived Surface Temperature Distribution to Surface Temperature Derived from Sub-surface TC Measurement Using Inverse Methods

The left side of Figure 8-1 shows the temperature image for frame 7848 (note different color scale than that shown in Table 6-1) that has been rotated 90 deg counter-clockwise from that shown in Figure 2-1. The right side presents a temperature profile extracted across the dimensional temperature image. The diamond symbols represent the sub-surface temperatures derived from plug06 and plug08 TCs that have been extrapolated to the recessing heat shield surface. This process was performed at all five times the imagery was evaluated. The imagery estimates were consistently lower than the TC derived temperatures (see Ref. 21). Most of the differences were in the range of 100 °F. The relatively small lateral temperature gradients derived from the heat shield imagery would not account for the large bias. It was determined that a spectral emissivity value of approximately 0.55 would be required to drive the image derived temperatures to the values of the TC measurements. This emissivity value is not supported by any laboratory measurement. Because of the reconstruction process and the non-physical reading of several of the other near surface TCs, comparison of the image derived surface temperature to other measurements at TC locations were not attempted. At the time of this paper publication, the EFT-1 heat shield TC reconstruction process is in the early iterative stages of modeling updates and uncertainties have not been fully evaluated.

Interestingly, the temperature time history for plug08 was compared to the temperature time history derived from the imagery (see Ref. 36). The resulting linear slopes, Figure 9-2 correlated extremely well, indicating the temperature change, or cooling rate, was accurately captured by both measurement methods. In summary, the total uncertainty of the observation based temperature (±15 °F) is significantly smaller than the observed ~100 °F temperature difference between the two measurement techniques. Even a simple addition of the various contributors to uncertainties

in the imagery estimates discussed earlier would only yield a ±30 °F uncertainty. This bias cannot be explained by the uncertainties identified in the factors driving the observation-based temperature. However, the cooling rates inferred from the two measurements were consistent. This suggests further examination into the TC reconstruction process should be considered, including a high-fidelity uncertainty analysis of the charred and ablated Avcoat™ material properties.

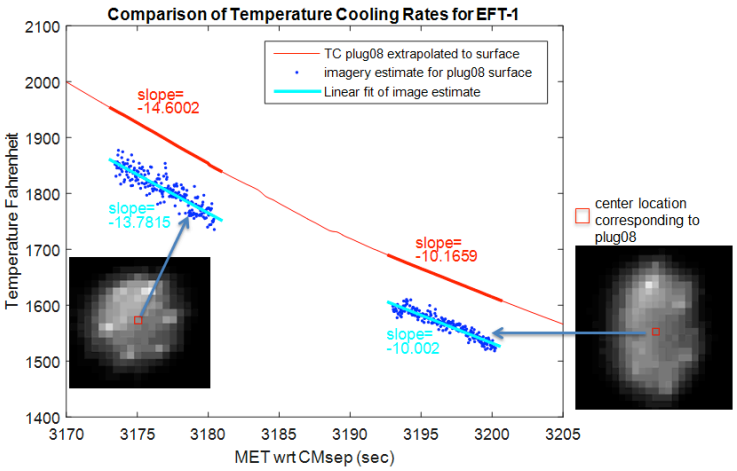

Figure 9-2. Comparison of Temperature Cooling Rates during Two Selected Intervals of Reentry When Best Imagery was Acquired

10. Concluding Remarks

A comprehensive assessment was undertaken by the NESC to determine the viability of quantitative thermal imaging of the Orion capsule heat shield during its reentry. While quantitative thermal imaging was successfully demonstrated on the Shuttle Orbiter, the Orion EFT-1 capsule presented unique challenges to the observation and analysis teams. The higher entry velocity and ablating heat shield required the team to assess the potential impact of shock layer radiation and ablation on the imaging quality. In contrast to the Shuttle observations, the capsule would be at exoatmospheric conditions as it came over the horizon into view of the imaging aircraft. As a result, a significantly weaker thermal signature of the capsule was presented to the sensor operator. Pre-mission radiance modeling provided advance situational awareness on how to optimally configure the imaging system for the expected weak thermal signature during initial long-range acquisition and the much stronger signature as the capsule passed by the aircraft at closest approach. Logistics of executing the observation campaign were presented. During the time of reentry, high altitude obscuring clouds were present at the planned imaging site. Precise communication between the mission operations team and the flight crew and the instrument operators were required to reposition the aircraft down range for a successful observation.

The imaging team successfully acquired the Orion capsule and observed it for over 60 seconds during hypersonic reentry. Approximately 900 unsaturated NIR images were obtained as the capsule decelerated from Mach numbers of 9.9 to 7.6. Image processing techniques were highlighted that increased the effective spatial resolution of the imagery and the overall signal to noise. Sensor calibration permitted the infrared intensity measurements to be converted to global surface temperature. The resulting surface temperature images will serve as an independent measurement for evaluating the performance of embedded in-situ thermocouples. The direct comparison of the mage-derived surface temperatures with surface temperatures inferred from reconstructed methods were made. An uncertainty analysis of the imagery suggests the observed temperature difference of approximately 100 °F could be attributed to uncertainties in the inverse heating response model. Additional work to refine the error estimates of both measurement techniques will lead to a better understanding of the aerothermal environment during high-speed reentry.

Acknowledgements

The authors would like to gratefully acknowledge the numerous behind the scenes team members not mentioned as their contributions were a large part of the team's success. For their outstanding efforts, the NASA Engineering and Safety Center presented the team with a Group Achievement Award in 2015.

10. References

[1] NESC Assessment: Orbiter Boundary Layer Transition (BLT) Testing for Development of Aeroheating Prediction Methodology, Task 5: Remote Entry Imaging (Phase A), NESC-TI-07-00413.

[2] Horvath, T.; Berry, S.; Alter, S.; Blanchard, R.; Schwartz, R.; Ross, M.; and Tack, S.: "Shuttle Entry Imaging Using Infrared Thermography," AIAA-2007-4267, June 2007.

[3] Ross, M.; Werner, M.; Mazuk, S.; Blanchard, R.; Horvath, T.; Berry, S.; Wood, W.; and Schwartz, R.: "Infrared Imagery of the Space Shuttle at Hypersonic Entry Conditions," AIAA-2008-0636, *46th AIAA Aerospace Sciences Meeting and Exhibit*, Reno, NV, January 7–10, 2008.

[4] Schwartz, R.; Ross, M.; Baize, R.; Horvath, T.; Berry, S.; and Krasa, P.: "A System Trade Study of Remote Infrared Imaging for Space Shuttle Re-entry," AIAA-2008-4023, June 2008.

[5] Splinter, S.; Daryabeigi, K.; Horvath, T.; Mercer, C. D.; Ghanbari, C.; Tietjen, A.; and Schwartz, R.: "Solar Tower Experiments for Radiometric Calibration and Validation of Infrared Imaging Assets and Analysis Tools for Entry Aero-Heating Measurements," AIAA-2008-4025, June 2008.

[6] Horvath, T.; Berry, S.; Splinter, S.; Daryabeigi, K.; Wood, W.; Schwartz, R.; and Ross, M.: "Assessment and Mission Planning Capability For Quantitative Aerothermodynamic Flight Measurements Using Remote Imaging," AIAA-2008-4022, June 2008.

[7] Berry, S.; Horvath, T.; Schwartz, R.; Ross, M.; Campbell, C.; and Anderson, B.: "IR Imaging of Boundary Layer Transition Flight Experiments," AIAA-2008-4026, June 2008.

[8] Gibson, D. M.; Spisz, T. S.; Taylor, J. C.; Zalameda, J. N.; Horvath, T. J.; Tomek, D. M.; Tietjen, A. B.; Tack, S.; and Bush, B. C.: "HYTHIRM Radiance Modeling and Image Analyses in Support of STS-119, STS-125, and STS-128 Space Shuttle Hypersonic Re-entries," AIAA Paper 2010-244, January 2010.

[9] Zalameda, J. N.; Horvath, T. J.; Tomek, D. M.; Tietjen, A. B.; Gibson, D. M.; Taylor, J. C.; Tack, S.; Bush, B. C.; Mercer, C. D.; and Shea, E. J.: "Application of a Near Infrared Imaging System for Thermographic Imaging of the Space Shuttle during Hypersonic Re-entry," AIAA Paper 2010-245, January 2010.

[10] Tack, S.; Tomek, D. M.; Horvath, T. J.; Verstynen, H. A.; and Shea, E. J.: "Cast Glance Near Infrared Imaging Observations of the Space Shuttle during Hypersonic Re-entry," AIAA Paper 2010-243, January 2010.

[11] Horvath, T. J.; Tomek, D. M.; Berger, K. T.; Splinter, S. C.; Zalameda, J. N.; Krasa, P. W.; Tack, S.; Schwartz, R. J.; Gibson, D. M.; and Tietjen A. B.: "The HYTHIRM Project: Flight Thermography of the Space Shuttle during Hypersonic Re-entry," AIAA Paper 2010-241, January 2010.

[12] Spisz, T. S.; Taylor, J. C.; Gibson, D. M.; Kwame, O. W.; Horvath, T. J.; Zalameda, J. N.; Tomek, D. M.; Berger, Tietjen, A. B.; Tack, S.; and Schwartz, R. J.: "Processing near-infrared imagery of hypersonic space shuttle reentries," *Thermosense XXXII Conference at 2010 SPIE Defense, Security, and Sensing Symposium*, April 5–9, 2010, Orlando, FL, Paper#7661-17.

[13] Taylor, J. C.; Spisz, T.; Kennerly, S.; Gibson, D.; Horvath, T.; Zalameda, J.; Splinter, S.; Kerns, R.; and Schwartz, R.: "Global Thermography of the Space Shuttle during Hypersonic Re-entry," AIAA 2011-3324, June 2011.

[14] Schwartz, R. J.; McCrea, A. C.; Gruber, J. R.; Hensley, D. W.; Verstynen, H. A.; Oram, T.; Berger, K. T.; Splinter, S.; Horvath, T. J.; and Kerns, R. V.: "Remote Infrared Imaging of the Space Shuttle During Hypersonic Flight: HYTHIRM Mission Operations and Coordination," AIAA 2011-3326, June 2011.

[15] Horvath, T. J.; Kerns, R. V.; Jones, K. M.; Grinstead, J. H.; Schwartz, R. J.; Gibson, D. M.; Tack, S.; and Dantowitz, R. F.: "A Vision of Quantitative Imaging Technology for Validation of Advanced Flight Technologies," AIAA-2011-3325, June 2011.

[16] Horvath, T. J.; Zalameda, J. J.; Wood, W. A.; Berry, S. A.; Swartz, R. J.; Dantowitz, R. F.; Spisz, T. S.; and Taylor, J. C.: "Time Resolved Global Infrared Observations of Roughness Induced Boundary Layer Transition on the Space Shuttle Orbiter During STS-134 Reentry," NATO RTO-MP-AVT-200-27, *Applied Vehicle Technology Panel and Specialist's meeting on Hypersonic Laminar-Turbulent Transition*, San Diego, CA, April 16–19, 2012.

[17] Spisz, T. S.; Taylor, J. C.; Gibson, D. M.; Kennerly, S. W.; Kwame, O.; Horvath, T. J.; Zalameda, J. N.; Kerns, R. V.; Shea, E. J.; Mercer, C. D.; Schwartz, R. J.; Dantowitz, R. F.; and Kozubal, M. J.: "Processing Ground-Based Near-Infrared Imagery of Space Shuttle Reentries," *Thermosense XXXIV Conference at 2012 SPIE Defense, Security, and Sensing Symposium*, April 23–27, 2012, Baltimore, MD, Paper 8354-15.

[18] Zalameda, J. N.; Horvath, T. J.; Kerns, R. V.; Taylor, J. C.; Spisz, T. S.; Gibson, D. M.; Shea, E. J.; Mercer, C. D.; Schwartz, R. J.; Tack, S.; Bush, B. C.; and Dantowitz, R. F.: "Thermographic Imaging of the Space Shuttle during Re-Entry Using a Near Infrared Sensor," *Thermosense XXXIV Conference at 2012 SPIE Defense, Security, and Sensing Symposium*, April 23-27, 2012, Baltimore, MD, Paper 8354-14.

[19] Horvath, T. J.; Cagle, M. F.; Grinstead, J. H.; and Gibson, D. M.: "Remote Observations of Reentering Spacecraft Including the Space Shuttle Orbiter," IEEE-2013-2707, March 2013.

[20] Morring, F., Jr.: "NASA, SpaceX Share Data On Supersonic Retropropulsion," *Aviation Week & Space Technology*, October 20, 2014.

[21] NESC Assessment: Remote Imaging of Exploration Flight Test-1 (EFT-1) Entry Heating Risk Reduction, NESC-RP-12-00795, May, 2016.
[22] Berger, K. T., Anderson, B. P., Campbell, C. H., Garske, M. T., Saucedo, L. A., Kinder, G. R., and Micklos, A. M., "Boundary Layer Transition Flight Experiment Overview," 42nd AIAA Thermophysics Conference, American Institute of Aeronautics and Astronautics, Reston, VA, AIAA-2011-3323, June 2011.
[23] Anderson, B., Campbell, C., Kinder, J., Saucedo, L., "Boundary Layer Transition Flight Experiment Overview and In-Situ Measurements," AIAA-2010-240, January 2010.
[24] Oliver, A. B., Amar, A. J., Droba, J., Lessard V., Mahzari, M. "EFT-1 Heatshield Aerothermal Environment Reconstruction", 46th AIAA Thermophysics Conference; 13-16 Jun. 2016; Washington, DC.
[25] Oliver, A. B., Amar, A. J., "Inverse Heat Conduction Methods in the CHAR Code for Aerothermal Flight Data Reconstruction", 46th AIAA Thermophysics Conference; 13-16 Jun. 2016; Washington, DC.
[26] Supporting Aerothermal Data for EFT-1 90-Day Post Flight Report, Orion, Multi Purpose Crew Vehicle (MPCV) Aerothermodynamics Team, NASA JSC, March, 2015.
[27] Schwartz, R. J., McCrea, A. C., "Virtual Diagnostic Interface: Aerospace Experimentation In The Synthetic Environment," MODSIM World Conference and Expo., Oct., 14, 2009.
[28] Schwartz, R.J., "ViDI: Virtual Diagnostics Interface Volume 1-The Future of Wind Tunnel Testing" Contractor Report NASA/CR-2003-212667, December 2003.
[29] Schwartz, R.J., Fleming, G.A.,"LiveView3D: Real Time Data Visualization for the Aerospace Testing Environment", AIAA-2006-1388, 44th AIAA Aerospace Sciences Meeting and Exhibit, Reno, Nevada, Jan. 9-12, 2006.
[30] Crow, D.; Coker, C.; and Keen, W.: "Fast Line-of-Sight Imagery for Target and Exhaust-Plume Signatures (FLITES) Scene Generation Program," Technologies for Synthetic Environments: Hardware-in-the-Loop Testing XI. Edited by Murrer, and Robert Lee, Jr., *Proceedings of the SPIE*, Volume 6208, June 2006.
[31] Oguz, H. N.; and O'Neil, J. M.: "EZMSLRAD Users Manual," JHU/APL, A1C-04-067, May 13, 2004.
[32] Berk, A.; Bernstein, L. S.; and Robertson, D. C.: "MODTRAN: A moderate resolution model for LOWTRAN7," Report GL-TR-89-0122, Air Force Geophys. Lab., Bedford, MA, April 1989.
[33] Kelly, M. A.; Osei-Wusu, K.; Spisz, T. S.; Strong, S.; Setters, N.; and Gibson, D. M.: "Assimilation of nontraditional datasets to improve atmospheric compensation," *2012 SPIE Defense Security & Sensing Symposium, Atmospheric Propagation IX*, SPIE-8380.
[34] "Standard Plume Ultraviolet Radiation Code (SPURC2.0) User's Manual," Air Force Research Lab, Edwards AFB, CA 93524, AFRL/PRSA-PS, January 2007.
[35] Whiting, E.; Park, C.; Liu, Y.; Arnold, J.; and Paterson, J.: "NEQAIR96, Nonequilibrium and Equilibrium Radiative Transport and Spectra Program: User's Manual," NASA RP-1389, 1996.
[36] Spisz, T. S., Taylor, J. C., Gibson, D. M., Kennerly, S., Kwame Osei-Wusu., Horvath, T. J., Schwartz, R. J., Tack, S., Bush, B. C., and Oliver, B., "Processing Near-Infrared Imagery of the Orion Heatshield During EFT-1 Hypersonic Reentry," AIAA-2016-xxx, June 2016.
[37] Santos, J.; Oishi, T.; and Martinez, E.: "Isotherm Sensor Calibration Program for Mars Science Laboratory Heat Shield Flight Data Analysis," *42nd AIAA Thermophysics Conference*, June 27–30, 2011, Honolulu, Hawaii, AIAA 2011-3955.
[38] Oliver, A. B.; Amar, A. J.; Droba, J.; Lessard V.; and Mahzari, M.: "EFT-1 Heatshield Aerothermal Environment Reconstruction," *46th AIAA Thermophysics Conference*; June 13–16, 2016, Washington, DC.
[39] Oliver, A. B.; and Amar, A. J.: "Inverse Heat Conduction Methods in the CHAR Code for Aerothermal Flight Data Reconstruction," *46th AIAA Thermophysics Conference*; June 13–16, 2016; Washington, DC.